Case Studies in Chemical and Environmental Engineering 9 (2024) 100562

Contents lists available at ScienceDirect

Case Studies in Chemical and Environmental Engineering

journal homepage: www.sciencedirect.com/journal/case-studies-in-chemical-and-environmental-engineering

Case Report

Nanostarch based nanoencapsulation of *Mucuna pruriens* extract and its evaluation as anti-parkinsonian drug

Ratnaningsih Eko Sardjono [a,*], Ramdhan Gunawan [a], Asep Kadarohman [a], Erdiwansyah [b,c,**], Rizalman Mamat [c], Melati Khairuddean [d]

[a] Chemistry Program, Universitas Pendidikan Indonesia, Setiabudi 229, Bandung, 40154, Indonesia
[b] Faculty of Engineering, Universitas Serambi Mekkah, Banda Aceh, 23245, Indonesia
[c] Centre for Automotive Engineering, Universiti Malaysia Pahang, 26600, Pekan, Malaysia
[d] School of Chemical Sciences, Universiti Sains Malaysia, 11800, Penang, Malaysia

ARTICLE INFO

Keywords:
Anti–Parkinson
Mucuna pruriens
Nanoencapsulation
Nanostarch
Parkinson's disease

ABSTRACT

Parkinson's disease is a neurodegenerative disease caused by low dopamine levels in the brain. This study aims to obtain the optimum condition for *M. pruriens* extract nanoencapsulation in nano starch (NS-MPn) and nanostarch-maltodextrin (NS-MD-MPn), nanocapsules characteristics, and their potential as anti-Parkinsonian drug. The nanoencapsulation process was carried out by ultrasonic method. FTIR, SEM, and TEM carried out the characterization of NS-MPn and NS-MD-MPn nanocapsules. Encapsulation efficiency was evaluated by UV-Vis spectroscopy. SEM and TEM characterization NS-MPn and NS-MD-MPn nanocapsules have non-spherical surface morphology, spherical in shape 234.98 and 90.85 nm, respectively. NS-MPn have 21.35% encapsulation efficiency, meanwhile, NS-MD-MPn has 30.02%.

1. Introduction

Parkinson's disease is one of the progressive neurodegenerative diseases. This disease can occur due to the damage of dopaminergic nerve cells in the brain. Damage to dopaminergic nerve cells can lead to a decrease in dopamine production, which disrupts the coordination system, such as movement [1]. The reduction of dopamine occurs in the substantia nigra compacta (SNc) of the brain [2]. About 10 million people are estimated to have suffered from Parkinson's disease. Parkinson's disease is mainly sustained by patients over the age of 60 years [3,4].

There are several approaches commonly used for the management of Parkinson's disease, such as therapy using dopamine precursors (levodopa), dopamine agonists, MAO-B inhibitors (monoamine oxidase-B), COMT inhibitors (catechol-O-methyltransferase), amantadine, and adenosine A2a antagonists [5]. Furthermore, there are several instrumental treatment options for Parkinson's disease such as Deep Brain Stimulation (DBS), thalamotomy, pallidotomy, lesion surgery, and neural grafting or tissue transplant. These six instrumental options aim to manage the motor symptoms of Parkinson's disease and enhance the quality of life for patients [6]. However, the six instrumental treatment options for Parkinson's disease, while effective in managing symptoms, are invasive and can lead to side effects such as dyskinesia, depression, cognitive changes, and speech problems [7–9]. Currently, treating Parkinson's disease using levodopa has become the most effective treatment and lower side effect compared to other therapies [10].

Mucuna pruriens (L.) DC. contains important phytochemical compounds such as alkaloids, tannins, proteins, xylitol, ascorbic acid, and levodopa. Therefore, *M. pruriens* has extensive pharmacological potential such as it can be an anti-venom, anti-microbial, anti-diabetic, anti-oxidant, and neuroprotective agent for Parkinson's disease [11–13]. However, some limitations of herbal medicine such as M. pruriens extract include low solubility in water, low bioavailability, and poor stability [2].

Nanomedicine represents an innovative field that combines two vastly different disciplines: nanotechnology and medicine. Nanotechnology involes the manipulation of matter on a nanometer scale (1–100 nm), while medicine deals with the treatment, diagnosis, and prevention of diseases [14]. More than 250 health-focused nanotechnology products are available in the market, and there are currently over 1500

* Corresponding author.
** Corresponding author. Faculty of Engineering, Universitas Serambi Mekkah, Banda Aceh, 23245, Indonesia.
E-mail addresses: ratnaeko@upi.edu (R.E. Sardjono), erdiwansyah5@gmail.com (Erdiwansyah).

https://doi.org/10.1016/j.cscee.2023.100562
Received 12 August 2023; Received in revised form 16 November 2023; Accepted 22 November 2023
Available online 26 November 2023

nanomedicine research projects ongoing worldwide. It is estimated that in 2020, the global market of nanomedicine was valued at $141.34 billion in 2020 and is projected to reach $258.11 billion bu 2025 [15]. Nanoparticles can be engineered to target specific cells or tissues and it can improve the solubility and stability of drugs, which can increase the effectiveness of drugs, reducing side effects and enhance its bioavaibility [16]. However, there are several disadvantages of nanomedicine, including the potential toxicity of some nanoparticles that could harm to patients, challenges in nanomedicine regulations, and the high costs of development and production [14,17].

The nanotechnology approach through the biodegradable matrices-based nanoencapsulation process can overcome these limitations. The nanoencapsulation formulation of this herbal medicinal compound is considered to have several advantages, such as having a larger contact surface area, a more targeted drug delivery system, more regulated release of drugs, and having high bioavailability and stability to increase the therapeutic effect [18,19]. Nanostarch has been widely used for the nanoencapsulation of several active compounds such as curcumin [20–23], piperine [24], catechin [25–27], epicatechin, epigallocatechin, epigalocatechin-3-galate, proanthocyanidine [27], and resveratol [28].

Recently, nanostarch has attracted a lot of researcher's attentions in various fields, especially in the pharmaceutical field. Nanostarch shows good physical and chemical properties such as having a high surface area, aspect ratio, and crystallinity; non-toxic and has good rheological properties, biodegradability, and water absorption ability to increase the effectiveness of the use of herbal medicines [29–34].

In this study, *M. pruriens* extract was encapsulated in nanostarch and nano starch-maltodextrin through an ultrasonic method. Nanostarch-*Mucuna pruriens* nanocapsule (NS-MPn) nanocapsules and nanostarch-maltodextrin-*Mucuna pruriens* nanocapsule (NS-MD-MPn) were characterized by FTIR, SEM, and TEM. A UV-Vis spectrometer determined the encapsulation efficiency. The potential anti-Parkinson's activity of nanocapsules was evaluated through catalepsy tests horizontal bar model.

2. Methods

2.1. M. pruriens extraction

M. pruriens seeds were obtained from Bantul, Yogyakarta and washed with water. The seeds were sun-dried for three days. Dried *M. pruriens* seeds were crushed and powdered. Extraction of *M. pruriens* seeds was carried out by the maceration method described by Sardjono et al. [35] with slight modifications. Briefly, 12 kg of *M. pruriens* seed powder was macerated in 12.5 L of ethanol: water (1: 1) for three days with daily solvent changes in 3 × 24 h. *M. pruriens* extract filtrate was obtained by filtration through Whatman filter paper 1. The filtrate was evaporated by a rotary evaporator. During the extract concentration process in rotary evaporator, the flask containing the extract was immersed in a water bath at 50 °C for approximately 90 minutes for single evaporation cycle. Each evaporation cycle used approximately 500 mL of filtrate. The concentrated extract was dried by freeze-drying method for 24h. The freezing temperature was set to −20 °C and freeze-drying pressure was set to be below 8 bar to maintain the appropriate vacuum conditions. The dry *M. pruriens* extracts were stored at 4 °C for further use.

2.2. Determination of levodopa content in M. pruriens extract

The levodopa content in *M. pruriens* extract was analysed by Hitachi D7000 High-Performance Liquid Chromatography (HPLC) with UV detector and C-18 column 250 × 4.6 mm. The mobile phase consisted of water, methanol, and phosphoric acid (97 ml: 20 ml: 1 ml) with pH of 5–7, and the flow rate was 1 mL/min. The detection was carried out under UV detector at 280 nm. 12.5 mg of levodopa standard was dissolved in a 25 mL mobile phase to obtain a 500-ppm primary standard solution. Series of traditional solutions prepared in 25, 50, 75, 100, 125 and 150 ppm concentrations. 12.5 mg of *M. pruriens* extract was dissolved in 25 mL of mobile phase to obtain a 500 ppm M. *pruriens* extract solution. The determination of levodopa content in *M. pruriens* extract was calculated through the calibration curve equation of the standard levodopa solution.

2.3. Nanostarch synthesis

Nanostarch was synthesized from soluble starch (Merk) by the acid hydrolysis method described by Kim et al. [36] with slight modification. Briefly, 30 g of starch was dispersed in 200 mL of 3.5 M sulfuric acid. Hydrolysis was carried out at 40 °C for 10 hours. The nanostarch suspension was obtained by centrifugation at 1663×*g* in 25 °C for 40 minutes. The nanostarch rest was neutralized by 1 M NaOH. The break was redispersed in 300 mL of distilled water and centrifuged at 1663×*g* in 25 °C for 40 minutes. The nanostarch suspension was oven-dried at 40 °C for 5–7 h.

2.4. M. pruriens nanoencapsulation in nanostarch

Nanoencapsulation of *M. pruriens* extract in nanostarch was carried out by the ultrasonic method described by Monterroza and Gutierrez [37] with slight modification. The *M. pruriens* extract solution (water,n g/100 mL) was added to nanostarch dispersion (water, n g/100) in 1g: 1g: 2g: 1g, 3g: 1g, 1g: 2g, and 1g: 3g (NS:MP) ratios. The mixture was sonicated (Ultrasonic Cell Disruption, UCD-250, probe temperature 24 °C, power rate 62%, pulse on 1 s, pulse off 1 s) for 1 h to produce NS-MPn nanocapsules. The NS-MPn suspension was obtained by centrifugation for 30 minutes at 1663×*g* in 25 °C and oven-dried 40 °C for 5–7 h. The NS-MPn nanocapsules were stored at 4 °C for further use.

2.5. M. pruriens nanoencapsulation in nanostarch-maltodextrin

Nanoencapsulation of *M. pruriens* extract in nano starch-maltodextrin was carried out by the ultrasonic method described by Monterroza and Gutierrez [37] with slight modification. The *M. pruriens* extract solution (water, n g/100 mL) was added to nano starch-maltodextrin dispersion (water, n g/100 mL) in 1g: 1g. 2g: 1g, 3g:1g, 1g: 2g, and 1g: 3g (NS-MD:MP) ratios. The mixture was sonicated (Ultrasonic Cell Disruption, UCD-250, probe temperature 24 °C, power rate 62%, pulse on 1 s, pulse off 1 s) for 1 hour to produce NS-MD-MPn nanocapsules. The NS-MD-MPn suspension was obtained by centrifugation for 30 minutes at 1663×*g* in 25 °C and oven-dried at 40 °C for 5–7 h. The NS-MD-MPn nanocapsules were stored at 4 °C for further use.

2.6. Characterization

Characterization was carried out by several instruments such as Fourier Transform Infra-Red (FTIR Shimadzu 8400), Scanning Electron Microscope (SEM Jeol JSM-IT3300) and Transmission Electron Microscope (TEM HT7700). FTIR analysis was conducted at Universitas Pendidikan Indonesia to determine the functional groups in *M. pruriens* extract, starch, nanostarch, NS-MPn nanocapsule, and NS-MD-MPn nanocapsule. SEM analysis was carried out at Lembaga Ilmu Pengetahuan, Indonesia, to determine the surface morphology of nanostarch, NS-MPn nanocapsules, and NS-MD-MPn nanocapsules. TEM analysis was conducted at Institut Teknologi Bandung to determine the shape and size of nanostarch, NS-MPn nanocapsules, and NS-MD-MPn nanocapsules.

For the FTIR analysis, the sample preparation is conducted using KBr pellet method, where the nanocapsules were mixed with KBr powder and pressed into a pellet for measurement by FTIR spectrometer. On the other hand, for TEM analysis, the sample is prepared by dispersing the nanocapsules in ethanol solvent. The dispersed sample is then applied to a TEM grid for the visualization and examination of the structure and morphology.

2.7. Encapsulation efficiency evaluation

Encapsulation efficiency was determined by UV-Vis spectrometry. The evaluation was conducted by establishing a calibration curve for the *M. pruriens* extract with a series of concentrations at 0 ppm, 5 ppm, 10 ppm, 15 ppm, and 20 ppm, measured at a wavelength of 280 nm. The absorption of the nanocapsules was measured at 280 nm, and the concentration of the active compound was determined using the calibration curve. The encapsulation efficiency was determined by subtracting the concentration of the total extract (Co) from the concentration of the unencapsulated extract (Ct) and dividing by the attention of the total quote (Co) as shown in the following (Eq. (1)).

$$Encapsulation\ efficiency(\%) = \frac{Co - Ct}{Co} x100\ \% \quad (1)$$

2.8. Evaluation of nanocapsules Anti-Parkinson activity

The anti-Parkinson's activity of NS-MPn and NS-MD-MPn nanocapsules was evaluated by catalepsy test using male Swiss webster mice, aged 2 months, with weights ranging from 20 to 30 g as described by Melo-Thomas and Thomas [38]. The mice were kept under standard conditions for 2 weeks and were provided with CP 511 feed and water. Briefly, mice were divided into four groups: standard control Pulvis Gummi Arabicum 1% (PGA), negative control (haloperidol 5 mg/kg), positive control (haloperidol 5 mg/kg + levodopa 10 mg/kg), and experimental control (haloperidol 5 mg/kg + *M. pruriens* extract 200 mg/kg or nanocapsules 5 mg/kg – 25 mg/kg. Each group consisted of 3 animals to ensure statistically significant results and reliable conclusions. 5 mg/kg of haloperidol dose has been found to effectively induce catalepsy in mice [39].

The catalepsy test was carried out through the horizontal bar test method [38,40]. The catalepsy test was carried out by administering samples dissolved in 1% PGA solution orally and haloperidol 5 mg/kg dissolved in 1% lactic acid through the intraperitoneal (I.P) route. The intensity of catalepsy time was measured by observing how long the mice lasted with both forelegs holding a 0.5 cm diameter bar without moving. Catalepsy was observed 30 minutes after the administration of haloperidol 5 mg/kg. Haloperidol was administered 30 minutes after oral administration of 1% PGA, NS-MPn and NS-MD-MPn nanocapsules at 5, 10, 15, 20, and 25 mg/kg doses, *M. pruriens* extract at 200 mg/kg dose, or L-DOPA at 10 mg/kg dose. The volume of drug administration given was adjusted according to the body weight of each mouse.

3. Result and discussion

3.1. FTIR spectra of M. pruriens extract

The functional groups present in the active compounds within *M. pruriens* seed extract were identified through FTIR spectroscopy. The FTIR spectrum shown in Fig. 1 reveals characteristic absorbances for vibrational stretching of O-H hydroxyl bonds at 3745.88 cm^{-1}, C-H at 2933.83 cm^{-1}, C-O at 2372.52 cm^{-1}, C=C at 2033.04 cm^{-1}, C=O at 1874.87 cm^{-1}, and C-N at 1610.61 cm^{-1}. Additionally, Fig. 1 also shows absorbances for the vibrational bending of O-H bonds at 1406.15 cm^{-1}, C-H at 929.72 cm^{-1}, C-O at 1062.81 cm^{-1}, C-N at 1116.82 cm^{-1}, and C-C at 812.06 cm^{-1}.

The same absorption patterns can also be found in the FTIR spectra of levodopa. This indicates that *M. pruriens* seed extract contains levodopa compounds. In addition to levodopa, based on the FTIR spectrum generated, *M. pruriens* seed extract shows indications of containing other secondary metabolite compounds such as alkaloids, fatty acids, amino acids, flavonoids, and phenols [41–46].

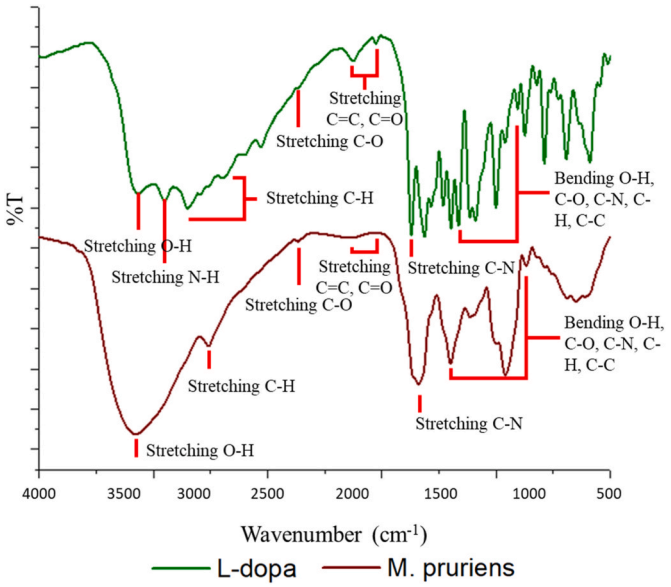

Fig. 1. FTIR spectra of *M. pruriens* extract, revealing the identification of various functional groups within the active compounds. The spectrum demonstrates characteristic absorbances, including vibrational stretching of O-H hydroxyl bonds at 3745.88 cm^{-1}, C-H at 2933.83 cm^{-1}, C-O at 2372.52 cm^{-1}, C=C at 2033.04 cm^{-1}, C=O at 1874.87 cm^{-1}, and C-N at 1610.61 cm^{-1}. The absorption pattern also signifies the vibrational bending of O-H bonds at 1406.15 cm^{-1}, C-H at 929.72 cm^{-1}, C-O at 1062.81 cm^{-1}, C-N at 1116.82 cm^{-1}, and C-C at 812.06 cm^{-1}. These findings suggest the presence of levodopa and other secondary metabolites such as alkaloids, fatty acids, amino acids, flavonoids, and phenols within the *M. pruriens* seed extract.

3.2. HPLC analysis of M. pruriens extract

Levodopa content in *M. pruriens* extract was determined by HPLC analysis. Fig. 2 shows the peak of levodopa standard chromatogram at the retention time of 1.71 minutes and chromatogram of *M. pruriens* extract at the retention time of 1.5; 1.59; 1.71; 2.88; 3.35; 4.17; and 4.84 minutes. Chromatogram at 1.71 minutes of retention time was used to determine the levodopa content in *M. pruriens* extract. Based on HPLC analysis, in 500 ppm, *M. pruriens* removed contained 27% levodopa.

3.3. Synthesis and characterization of nanostarch

The starch hydrolysis mechanism starts from the reaction of an acid proton with oxygen that binds two glucose units, followed by the cleavage of the C-O bond and the formation of a cyclic carbocation. 200 mL of water was added to stop the hydrolysis reaction, where sugar molecules would be formed, followed by the release of protons [47]. Hence, starch molecules would degrade to form smaller polysaccharides, producing nanostarch.

FTIR spectroscopy was conducted to see the effect of starch hydrolysis in the nanostarch synthesis process. The FTIR spectra in Fig. 3 show the typical absorption peaks for O-H, C-H, C-C, and C-O-C vibrations. According to M. Ahmad et al. [48], this spectra pattern represents the glucose units of amylose and amylopectin. In addition, it was also observed that the intensity of the absorption peak for C-O-C vibration in nanostarch decreased compared to soluble starch. This is caused by the reduction of glycosidic bonds in the glucose units of nanostarch due to hydrolysis [49]. The similarity of the two spectra shown indicates no change in the chemical structure of the glucose units of nanostarch.

SEM and TEM microscopy was used to observe the surface morphology, shape, and size of the nanostarch. The SEM image in Fig. 4A shows the synthesized nanostarch has a non-spherical morphology, and the TEM image in Fig. 4B shows the synthesized

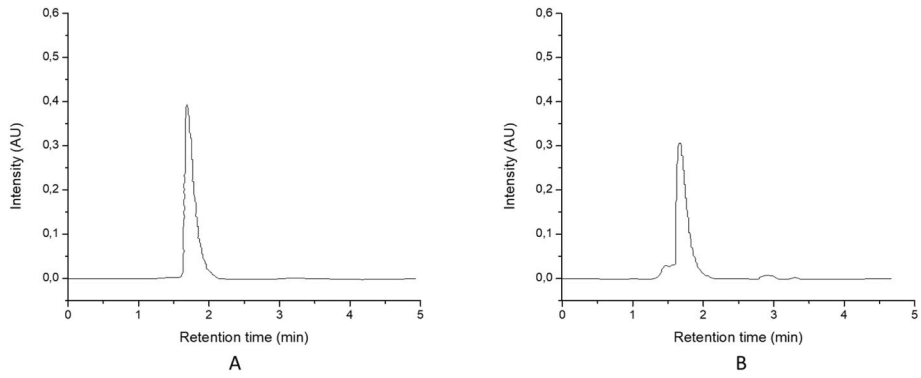

Fig. 2. HPLC chromatogram of levodopa and *M. pruriens* extract, The chromatogram displays the peak of levodopa at the retention time of 1.71 minutes, along with the chromatogram of *M. pruriens* extract indicating peaks at various retention times: 1.5, 1.59, 1.71, 2.88, 3.35, 4.17, and 4.84 minutes. The chromatogram at 1.71 minutes retention time was utilized to assess the levodopa content within the *M. pruriens* extract. The HPLC analysis revealed that the *M. pruriens* extract contained approximately 27% levodopa.

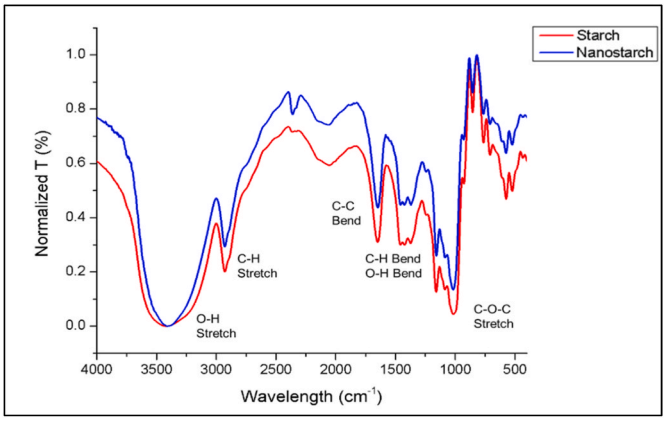

Fig. 3. FTIR spectra of starch and nanostarch, The spectra demonstrate characteristic absorption peaks for O-H, C-H, C-C, and C-O-C vibrations. These absorption patterns correspond to the glucose units of amylose and amylopectin. A noticeable decrease in the intensity of the absorption peak for C-O-C vibration in nanostarch compared to starch is observed, attributed to the reduction of glycosidic bonds in the glucose units of nanostarch. The similarity between the two spectra suggests no significant change in the chemical structure of the glucose units of nanostarch.

nanostarch is spherical with an average size of 226.5 nm.

3.4. Nanoencapsulation of M. pruriens extract

Nanostarch-based nanoencapsulation of *M. pruriens* extract includes nanoencapsulation by nanostarch and nano starch-maltodextrin. The addition of maltodextrin was conducted to see the effect of adding maltodextrin as a co-matrix to nanocapsules product. The maltodextrin used was 0.1 g. The nanoencapsulation process was carried out by mixing *M. pruriens* extract solution with nanostarch and nano starch-maltodextrin, respectively, in demineralized water and sonicated for 1 hour. During the ultrasonication process, acoustic cavitation occurs, causing the degradation of nanostarch and nano starch-maltodextrin polymers to produce smaller particles [50–53].

Optimization of the *M. pruriens* extract nanoencapsulation process was carried out by varying the composition of the extract, nanostarch, and nanostars-maltodextrin used. This optimization process aims to determine the optimal design to obtain more nanocapsules products. The results of nanoencapsulation optimization in Table 1 show that using more nanostarch and nano starch-maltodextrin can produce more nanocapsules. The composition of nanostarch and nanostars-maltodextrin: *M. pruriens* extract (3:1) yielded the most nanocapsules, 65.4% and 69.1%, respectively. Thus, it can be concluded that by increasing the amount of nanostarch/nanostarch-maltodextrin the weight amount of nanocapsules increases as well.

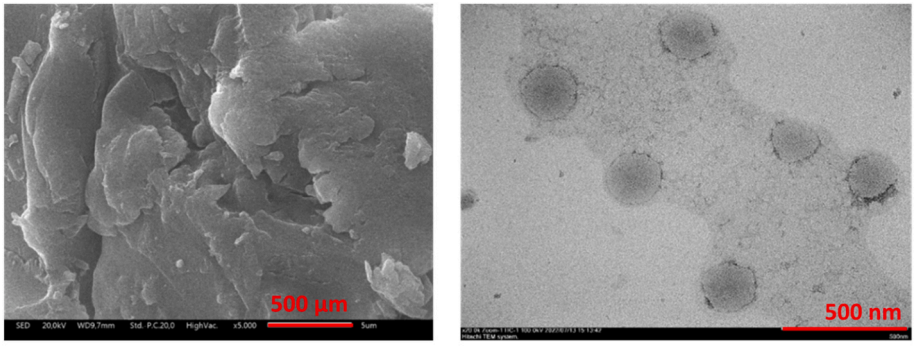

Fig. 4. SEM (A) and TEM (B) images of nanostarch, Depicting the surface morphology, shape, and size characteristics. The SEM image (A) illustrates that the nanostarch possesses a non-spherical morphology, while the TEM image (B) reveals that the synthesized nanostarch exhibits a spherical shape with an average size measuring 226.5 nm.

Table 1
Nanoencapsulation optimization.

Matrices: *M. pruriens*	NS-MPn nanocapsules		NS-MD-MPn nanocapsules	
	Weight (g)	Yield (%)	Weight (g)	Yield (%)
1: 1	0.08	39.8	0.13	43.6
2: 1	0.17	55.7	0.24	59.9
3: 1	0.26	65.4	0.35	69.1
1: 2	0.11	35.4	0.16	40.05
1: 3	0.13	31.7	0.20	40.32

3.5. Characterization of NS-MPn and NS-MD-MPn nanocapsules

Characterization of NS-MPn and NS-MD-MPn nanocapsules by FTIR spectroscopy was conducted to determine the interaction between the phytochemical of *M. pruriens* extract with nanostarch and nanostars-maltodextrin. The FTIR spectra in Fig. 5 show the formation of new absorptions of aromatic C=O and C=C vibrations at wave numbers 1645.33 cm^{-1} and 1643.31 cm^{-1} in the FTIR spectrum of nanocapsules.

These two absorption peaks indicated the presence of phytochemicals of *M. pruriens* extract, such as levodopa in NS-MPn and NS-MD-MPn nanocapsules. In addition, a shift in the O-H vibration was observed from the initial wave number of 3406.40 cm^{-1} in nanostarch to 3387.11 cm^{-1} for NS-MPn nanocapsules and 3394.83 cm^{-1} for NS-MD-MPn nanocapsules (Table 2). These absorption shifts are expected due to hydrogen interactions from phytochemicals of *M. pruriens* extract, such as levodopa with nanostarch and nanostars-maltodextrin (Fig. 6).

In addition, SEM and TEM analyses were conducted to observe the surface morphology, particle shape, and size of the NS-MPn and NS-MD-MPn nanocapsules. SEM images of NS-MPn and NS-MD-MPn nanocapsules in Fig. 7A and B show that nanocapsules have non-spherical surface morphology. The SEM images also showed that the nanocapsules have smooth surfaces. This smoothness can be indicative of a well-distributed coating of the *M. pruriens* extract within the nanostarch matrices, contributing to a more uniform and controlled release of the encapsulated material [54,55].

Meanwhile, TEM images of NS-MPn and NS-MD-MPn nanocapsules in Fig. 8 illustrate the *M. pruriens* extract's phytochemicals loading in nanocapsules as proposed by Refs. [56,57]. In addition, Fig. 8 shows both NS-MPn and NS-MD-MPn nanocapsules are spherical, regular, and monodispersed particles with average sizes of 234.9 nm and 90.9 nm, respectively. This suggests that the nanocapsules maintain a consistent and well-defined spherical structure, reinforcing the notion of uniformity in their shape and internal composition. This could potentially lead to uniform behavior of the nanocapsules, such as in their drug release profiles [58].

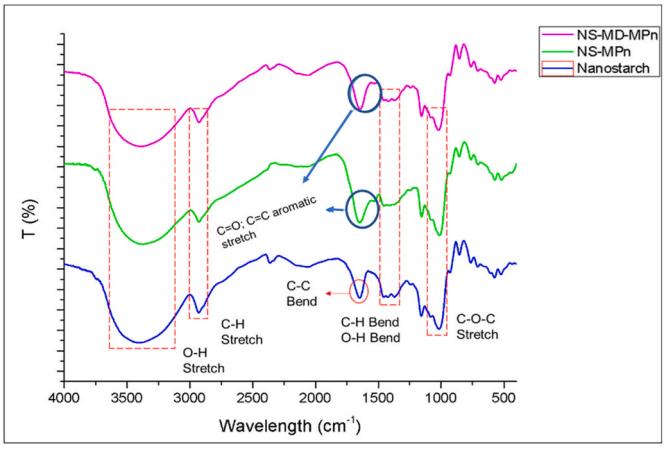

Fig. 5. FTIR spectra of nanostarch, NS-MPn, and NS-MD-MPn nanocapsules, Revealing the emergence of new absorptions of aromatic C=O and C=C vibrations at wave numbers 1645.33 cm^{-1} and 1643.31 cm^{-1}, respectively, in the FTIR spectrum of the nanocapsules. These two absorption peaks are indicative of the presence of phytochemicals from *M. pruriens* extract, including levodopa, within the NS-MPn and NS-MD-MPn nanocapsules.

Table 2
FTIR analysis of nanostarch, NS-MPn, and NS-MD-MPn nanocapsules.

Vibration	Wavelength (cm^{-1})		
	Nanostarch	NS-MPn	NS-MD-MPn
O-H stretch	3406,40	3387,11	3394,83
C-H stretch	2928,04	2929,97	2926,11
C-C bend	1645,33	1645,33–1600	1643,31–1600
C=O stretch	N/A	**1645,33**	**1643,31**
C=C aromatic stretch	N/A	**1600–1500**	**1600–1500**
C-H stretch	1456,30	1454,38	1456,30
O-H stretch	1369,50	1421,58	1419,66
C-O-C stretch	1016,52	1014,59	1020,38

N/A: not available

3.6. Encapsulation efficiency evaluation

Evaluation of the *M. pruriens* extract's encapsulation efficiency in nanostarch and nanostars-maltodextrin aimed to determine how much phytochemicals were encapsulated in the matrices. Evaluation of encapsulation efficiency was carried out by UV-Vis spectroscopy. The results of the encapsulation efficiency evaluation in Fig. 9 show that the phytochemicals encapsulated in nanostarch were 21.35% and in nanostars-maltodextrin was 30.02%. These results indicate that adding maltodextrin as a co-matrix can increase the amount of phytochemicals encapsulated in nanocapsules. This is because adding the co-matrix gives the extract phytochemicals more options to interact with the matrices.

3.7. Catalepsy test evaluation

The catalepsy test evaluation result in Table 3 shows that mice induced by haloperidol 5 mg/kg could not move or fix their position on the bar for 352.57 seconds compared to normal mice (0.55 seconds). This indicates that the mice experienced catalepsy, causing them to be unable to move or fix their position on the bar. The administration of haloperidol causes can cause dopaminergic D2 receptors in the nigrostriatal part of the mice to be blocked so that the mice experience catalepsy symptoms such as muscle stiffness. Hence, the mice could not move or fix their position on the bar [59,60].

Mice given levodopa 10 mg/kg experienced catalepsy for 33.1 seconds. This shows that administration of levodopa can reduce catalepsy symptoms significantly ($P < 0.05$). Mice that were given *M. pruriens* extract 200 mg/kg experienced catalepsy for 269.58 seconds. In addition, administration of NS-MPn and NS-MD-MPn nanocapsules at 5 mg/kg to 25 mg/kg doses can also reduce catalepsy symptoms in mice, and their activity was more significant than the administration of *M. pruriens* extract itself at 200 mg/kg dose. Thus, this shows that the administration of *M. pruriens* removes, NS-MPn, and NS-MD-MPn nanocapsules can significantly reduce catalepsy symptoms compared to negative controls ($P < 0.05$).

The ability of NS-MPn and NS-MD-MPn nanocapsules to reduce catalepsy symptoms was influenced by the dose given to mice, as shown in Fig. 10. The catalepsy-reducing activity conducted by nanocapsules tended to increase in larger quantities. In addition, NS-MD-MPn nanocapsules showed better catalepsy-reducing activity than NS-MPn nanocapsules. This is presumably due to the higher encapsulation efficiency of NS-MD-MPn nanocapsules so that more levodopa can be released. In addition, the smaller size compared to NS-MPn nanocapsules allows NS-MD-MPn nanocapsules to interact more effectively.

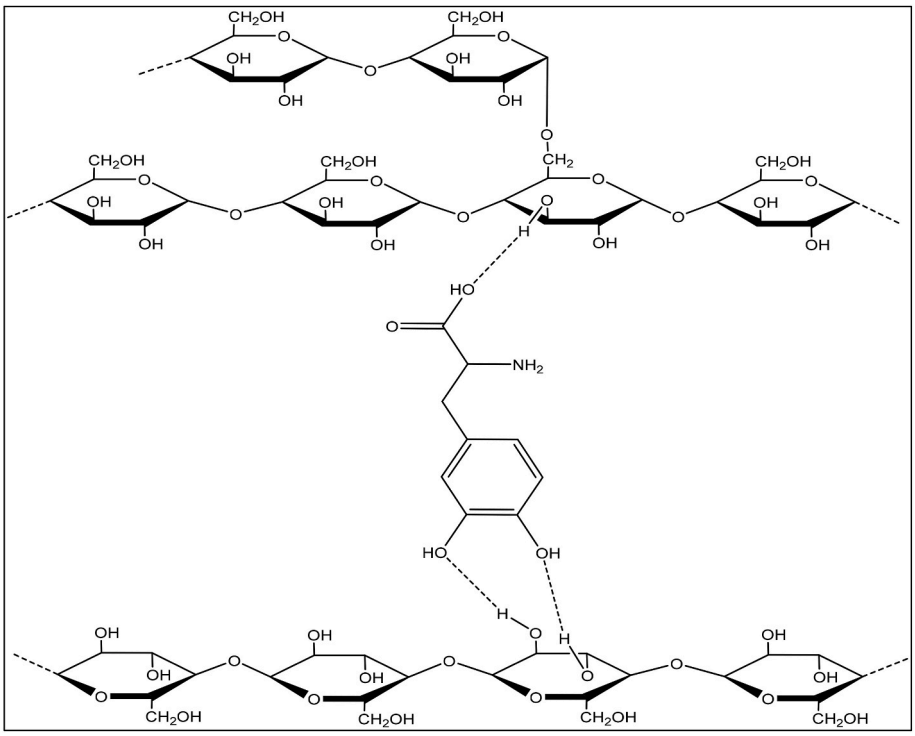

Fig. 6. Possible levodopa interaction in NS-MPn and NS-MD-MPn nanocapsules, Demonstrating the hydrogen interaction between phytochemicals such as levodopa in *M. pruriens* extract based on shifted O-H vibration from the initial wave number of 3406.40 cm^{-1} in nanostarch to 3387.11 cm^{-1} for NS-MPn nanocapsules and 3394.83 cm^{-1} for NS-MD-MPn nanocapsules.

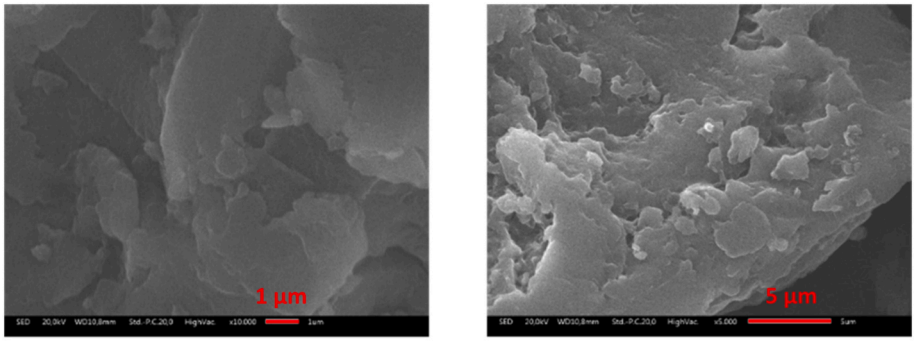

Fig. 7. SEM images of NS-MPn (A) and NS-MD-MPn (B), Revealing the non-spherical surface morphology of the nanocapsules observed in both NS-MPn and NS-MD-MPn.

4. Prospects

The prospects for the nanostars-based nanoencapsulation of Mucuna pruriens extract as an anti-Parkinsonian drug are exciting and hold potential for addressing several challenges associated with conventional treatments for Parkinson's disease. Here are some considerations for the future development and evaluation of this approach.

4.1. Improved therapeutic efficacy

Continued research and optimization of nano starch-based nanoencapsulation may improve therapeutic efficacy compared to traditional formulations. Fine-tuning the formulation can enhance active compounds' stability, bioavailability, and controlled release.

4.2. Targeted drug delivery

Advances in nanotechnology may allow for more precise targeting of affected areas in the brain associated with Parkinson's disease. Tailoring nanocarriers for specific cellular or tissue targets can enhance the delivery of therapeutic agents.

4.3. Combination therapies

The versatility of nanocarriers enables the possibility of combining Mucuna pruriens extract with other therapeutic agents or complementary treatments. This approach may provide a synergistic effect and address different aspects of Parkinson's disease pathology.

4.4. Personalized medicine

With further understanding of individual variations in response to

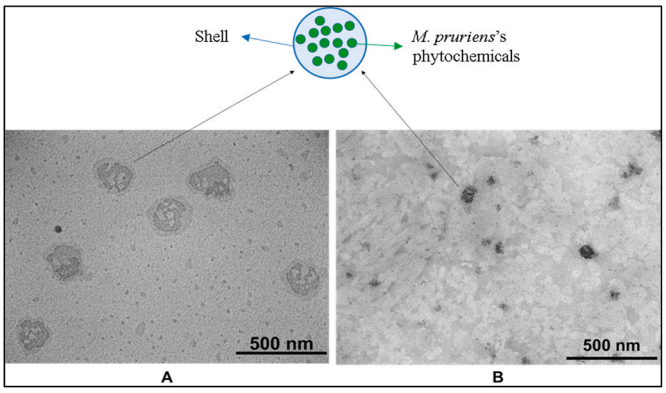

Fig. 8. TEM images of loaded NS-MPn (A) and NS-MD-MPn (B) nanocapsules, Indicating the loading of *M. pruriens* extract's phytochemicals within the nanocapsules. Both NS-MPn and NS-MD-MPn nanocapsules demonstrate a spherical shape, with average sizes measured at 234.9 nm and 90.9 nm, respectively.

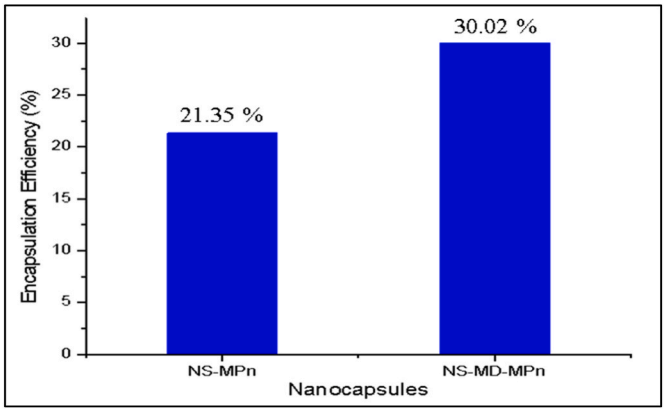

Fig. 9. Encapsulation efficiency of nanocapsules, illustrating that the phytochemicals encapsulated in nanostarch was 21.35%, while in nanostarch-maltodextrin, it was 30.02%. These results suggest that the addition of maltodextrin as a co-matrix can enhance the amount of phytochemicals encapsulated in the nanocapsules, likely due to the increased interaction between the extract's phytochemicals and the matrices.

Table 3
Catalepsy test evaluation.

Mice	Treatment	Catalepsy time (s)
Normal group	PGA 1 %	0.55 ± 0.32
Positive control	levodopa 10 mg/kg	33.1 ± 9.99
Negative control	Haloperidol 5 mg/kg	353.57 ± 68.56
Experiment control	*M. pruriens* extract 200 mg/kg	269.58 ± 20.04
	NS-MPn 5 mg/kg	220.91 ± 16.13
	NS-MD-MPn 5 mg/kg	220.83 ± 27.44
	NS-MPn 10 mg/kg	205.86 ± 9.66
	NS-MD-MPn 10 mg/kg	173.48 ± 30.98
	NS-MPn 15 mg/kg	188.49 ± 7.94
	NS-MD-MPn 15 mg/kg	133.47 ± 15.39
	NS-MPn 20 mg/kg	164.55 ± 21.83
	NS-MD-MPn 20 mg/kg	142.65 ± 17.12
	NS-MPn 25 mg/kg	146.36 ± 2.91
	NS-MD-MPn 25 mg/kg	117.43 ± 5.36

treatment, personalized formulations can be developed to meet the specific needs of patients. This could involve adjusting the composition and dosage of the nanoencapsulated formulation based on patient characteristics.

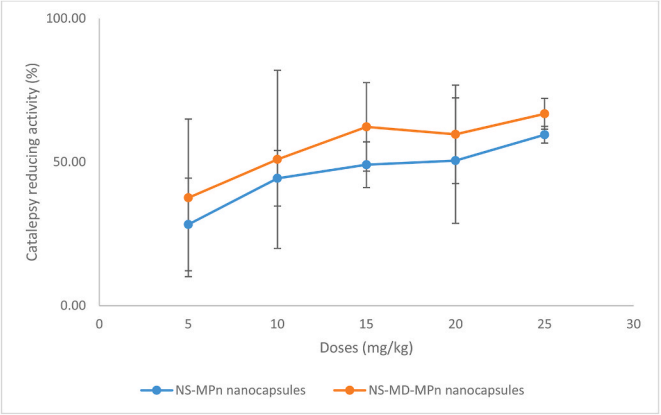

Fig. 10. Catalepsy-reducing activity of NS-MPn and NS-MD-MPn nanocapsules, Demonstrating the influence of dosage on the ability of the nanocapsules to reduce catalepsy symptoms in mice. The graph illustrates that the catalepsy-reducing activity generally increased with larger quantities administered. Notably, NS-MD-MPn nanocapsules exhibited more effective catalepsy reduction compared to NS-MPn nanocapsules, likely due to their higher encapsulation efficiency, leading to increased levodopa release. Moreover, the smaller size of NS-MD-MPn nanocapsules potentially allows for more effective interactions.

4.5. Long-term stability and safety

Future research should focus on ensuring the long-term stability and safety of nano starch-based nano encapsulation. Addressing potential biocompatibility, immunogenicity, and adverse effects concerns is crucial for developing a clinically viable treatment.

4.6. Smart drug delivery systems

Integrating intelligent drug delivery systems with responsive nanocarriers may enable real-time adjustments based on the patient's condition. These systems could adapt the release rate of therapeutic agents according to the progression of Parkinson's disease or individual responses.

4.7. Biomarker integration

Incorporating biomarkers into the evaluation process can provide valuable insights into the effectiveness of the treatment. Monitoring changes in relevant biomarkers may help assess disease progression and the impact of the nanoencapsulated formulation.

4.8. Regulatory approval and commercialization

Collaborative efforts between researchers, pharmaceutical companies, and regulatory agencies are essential for navigating the regulatory pathway. Addressing regulatory requirements early in the development process can expedite the approval and commercialization of the Nano encapsulated formulation.

4.9. Patient adherence and convenience

Consideration should be given to the ease of administration and patient adherence. Developing formulations that require less frequent dosing or have user-friendly administration methods can contribute to better patient compliance.

4.10. Global accessibility

Efforts should be made to ensure the developed Nano encapsulated

formulation is accessible globally, considering economic factors and healthcare infrastructure in different regions.

Continuous interdisciplinary collaboration, advancements in nanotechnology, and a comprehensive understanding of Parkinson's disease pathology will be crucial for the successful development and implementation of nano starch-based nanoencapsulation of Mucuna pruriens extract as an anti-Parkinsonian drug in the future.

5. Conclusion

Based on the research that has been done, the following conclusions are obtained: (1) The optimum conditions for the nanoencapsulation process of *M. pruriens* extract using both nanostarch and nanostars-maltodextrin matrices were obtained by ultrasonication method for 1 h and in matrices: *M. Pruriens* extract (3: 1) ratio, (2) NS-MPn and NS-MD-MPn nanocapsules have non-spherical surface morphology, spherical in shape, and have sizes of 234.98 nm and 90.85 nm respectively. The FTIR spectra showed new absorption peaks for C=C aromatic and C=O carbonyl vibrations indicating the *M. pruriens* phytochemicals' interaction with the matrices. NS-MPn nanocapsules have 21.35% encapsulation efficiency, NS-MD-MPn nanocapsules have 30.02% encapsulation efficiency, and (3) NS-MPn and NS-MD-MPn nanocapsules can significantly reduce catalepsy symptoms. The catalepsy-reducing activity the nanocapsules showed was more significant than the *M. pruriens* extract.

The results indicate that our optimized formulation exhibits enhanced efficacy in terms of improved bioavailability, thus presenting a more targeted and efficient therapeutic option. These findings underscore the potential of our method as a superior alternative in Parkinson's disease treatment, highlighting its role in revolutionizing the landscape of Parkinson's disease treatment. Further exploration and clinical validation of this approach are warranted to fully realize its impact on Parkinson's disease management.

CRediT authorship contribution statement

Ratnaningsih Eko Sardjono: Conceptualization, Data curation, Funding acquisition, Methodology, Validation. **Ramdhan Gunawan:** Data curation, Writing – original draft. **Asep Kadarohman:** Funding acquisition, Methodology, Resources, Visualization, Writing – review & editing. **Erdiwansyah:** Conceptualization, Data curation, Investigation, Validation, Conceptualization, Data curation, Investigation, Validation. **Rizalman Mamat:** Investigation, Methodology, Validation, Writing – review & editing. **Melati Khairuddean:** Methodology, Visualization, Writing – review & editing.

Declaration of competing interest

The authors declare that they have no known competing financial interests or personal relationships that could have appeared to influence the work reported in this paper.

Data availability

No data was used for the research described in the article.

References

[1] C.A. Lieu, K. Venkiteswaran, T.P. Gilmour, A.N. Rao, A.C. Petticoffer, E.V. Gilbert, M. Deogaonkar, B.V. Manyam, T. Subramanian, The antiparkinsonian and antidyskinetic mechanisms of Mucuna pruriens in the MPTP-treated nonhuman primate, Evidence-Based Complement, Altern. Med. (2012), https://doi.org/10.1155/2012/840247.

[2] S. Chatla, A. Obilineni, Nano Herbalmedicines (2021) 104–128.

[3] D. Aarsland, L. Batzu, G.M. Halliday, G.J. Geurtsen, C. Ballard, K. Ray Chaudhuri, D. Weintraub, Parkinson disease-associated cognitive impairment, Nat. Rev. Dis. Prim. 7 (2021) 47, https://doi.org/10.1038/s41572-021-00280-3.

[4] C. Marras, J.C. Beck, J.H. Bower, E. Roberts, B. Ritz, G.W. Ross, R.D. Abbott, R. Savica, S.K. Van Den Eeden, A.W. Willis, C.M. Tanner, on behalf of the P.F.P. Group, Prevalence of Parkinson's disease across north America, Npj Park. Dis 4 (2018) 21, https://doi.org/10.1038/s41531-018-0058-0.

[5] R. Pahwa, S. Swank, A Treatment Guide to Parkinson's Disease, 2020.

[6] V.D. Sharma, M. Patel, S. Miocinovic, Surgical treatment of Parkinson's disease: devices and lesion approaches, Neurotherapeutics 17 (2020) 1525–1538, https://doi.org/10.1007/s13311-020-00939-x.

[7] R.A. Barker, Neural transplants for Parkinson's disease: what are the issues? Poiesis Praxis 4 (2006) 129–143, https://doi.org/10.1007/s10202-006-0021-8.

[8] J.-Y. Li, W. Li, Postmortem studies of fetal grafts in Parkinson's disease: what lessons have we learned? Front. Cell Dev. Biol. 9 (2021).

[9] J. Rotter, G.R. Cosgrove, in: N. Pouratian, S.A. Sheth (Eds.), Parkinson's Disease: Lesions BT - Stereotactic and Functional Neurosurgery: Principles and Applications, Springer International Publishing, Cham, 2020, pp. 271–287, https://doi.org/10.1007/978-3-030-34906-6_19.

[10] H. Bogetofte, A. Alamyar, M. Blaabjerg, M. Meyer, Levodopa therapy for Parkinson's disease: history, current status and perspectives, CNS Neurol. Disord.: Drug Targets 19 (2020) 572–583, https://doi.org/10.2174/1871527319666200722153156.

[11] S. Divya, S. Kavimani, S.S. Rani, S. Subashree, S.P. Kumar, G. Mahalakshmi, T. Nirmala, R. Samundeswari, D. Sivassoupramanian, Parkinson's disease: a phytochemical approach, Int. J. Pharm. Rev. Res. (2014).

[12] P. Kurund, S. Gandla, Pharmacognostical, phytochemical and anti-Parkinson's profile of Mucuna pruriens, Res. J. Pharmacol. Pharmacodyn. (2021) 125–130, https://doi.org/10.52711/2321-5836.2021.00025.

[13] L.R. Lampariello, A. Cortelazzo, R. Guerranti, C. Sticozzi, G. Valacchi, The magic velvet bean of Mucuna pruriens, J. Tradit. Complement. Med. 2 (2012) 331–339, https://doi.org/10.1016/s2225-4110(16)30119-5.

[14] S. Soares, J. Sousa, A. Pais, C. Vitorino, Nanomedicine: principles, properties, and regulatory issues, Front. Chem. 6 (2018).

[15] T.J. Webster, Nanomedicine: Technologies and Applications, Woodhead Publishing, 2023.

[16] J.K. Patra, G. Das, L.F. Fraceto, E.V.R. Campos, M. del P. Rodriguez-Torres, L. S. Acosta-Torres, L.A. Diaz-Torres, R. Grillo, M.K. Swamy, S. Sharma, S. Habtemariam, H.-S. Shin, Nano based drug delivery systems: recent developments and future prospects, J. Nanobiotechnol. 16 (2018) 71, https://doi.org/10.1186/s12951-018-0392-8.

[17] S. Soliman, Nanomedicine: advantages and disadvantages of nanomedicine, 3 No: 666 1 Citation: Soliman S (2023), Rev. J Nanomed Nanotechnol. 14 (2023) 666, https://doi.org/10.35248/2157-7439.23.14.666.Citation.

[18] Y.D. Taghipour, M. Hajialyani, R. Naseri, M. Hesari, P. Mohammadi, A. Stefanucci, A. Mollica, M.H. Farzaei, M. Abdollahi, Nanoformulations of natural products for management of metabolic syndrome, Int. J. Nanomed. 14 (2019) 5303–5321, https://doi.org/10.2147/IJN.S213831.

[19] S. Noore, N.K. Rastogi, C. O'Donnell, B. Tiwari, Novel bioactive extraction and nano-encapsulation, Encycl. 1 (2021), https://doi.org/10.3390/encyclopedia1030052.

[20] G.K. Athira, A.N. Jyothi, Preparation and characterization of curcumin loaded cassava starch nanoparticles with improved cellular absorption, Int. J. Pharm. Pharmaceut. Sci. 6 (2014) 171–176.

[21] S.F. Chin, S.N.A. Mohd Yazid, S.C. Pang, Preparation and characterization of starch nanoparticles for controlled release of curcumin, Int. J. Polym. Sci. 2014 (2014), 340121, https://doi.org/10.1155/2014/340121.

[22] A. Maghsoudi, F. Yazdian, S. Shahmoradi, L. Ghaderi, M. Hemati, G. Amoabediny, Curcumin-loaded polysaccharide nanoparticles: optimization and anticariogenic activity against Streptococcus mutans, Mater. Sci. Eng., C 75 (2017) 1259–1267, https://doi.org/10.1016/j.msec.2017.03.032.

[23] M. Mani, M.K. Okla, S. Selvaraj, A. Ram Kumar, S. Kumaresan, A. Muthukumaran, K. Kaviyarasu, M.A. El-Tayeb, Y.B. Elbadawi, K.S. Almaary, B.M. Ahmed Almunqedhi, M.S. Elshikh, A novel biogenic Allium cepa leaf mediated silver nanoparticles for antimicrobial, antioxidant, and anticancer effects on MCF-7 cell line, Environ. Res. 198 (2021), 111199, https://doi.org/10.1016/j.envres.2021.111199.

[24] C. Wan-Hong, S. Chin, S.-C. Pang, K.-Y. Kok, Synthesis and characterisation of piperine-loaded starch nanoparticles, J. Phys. Sci. 31 (2020) 57–68, https://doi.org/10.21315/jps2020.31.1.4.

[25] M. Mani, R. Harikrishnan, P. Purushothaman, S. Pavithra, P. Rajkumar, S. Kumaresan, D.A. Al Farraj, M.S. Elshikh, B. Balasubramanian, K. Kaviyarasu, Systematic green synthesis of silver oxide nanoparticles for antimicrobial activity, Environ. Res. 202 (2021), 111627, https://doi.org/10.1016/j.envres.2021.111627.

[26] M. Ahmad, P. Mudgil, A. Gani, F. Hamed, F.A. Masoodi, S. Maqsood, Nano-encapsulation of catechin in starch nanoparticles: characterization, release behavior and bioactivity retention during simulated in-vitro digestion, Food Chem. 270 (2019) 95–104, https://doi.org/10.1016/j.foodchem.2018.07.024.

[27] C. Liu, S. Ge, J. Yang, Y. Xu, M. Zhao, L. Xiong, Q. Sun, Adsorption mechanism of polyphenols onto starch nanoparticles and enhanced antioxidant activity under adverse conditions, J. Funct.Foods 26 (2016) 632–644, https://doi.org/10.1016/j.jff.2016.08.036.

[28] M. Ahmad, A. Gani, Ultrasonicated resveratrol loaded starch nanocapsules: characterization, bioactivity and release behaviour under in-vitro digestion, Carbohydr. Polym. 251 (2021), 117111, https://doi.org/10.1016/j.carbpol.2020.117111.

[29] A.B. Perumal, R.B. Nambiar, J.A. Moses, C. Anandharamakrishnan, Nanocellulose: recent trends and applications in the food industry, Food Hydrocolloids 127 (2022), 107484, https://doi.org/10.1016/j.foodhyd.2022.107484.
[30] M.A. Odeniyi, O.A. Omoteso, A.O. Adepoju, K.T. Jaiyeoba, Starch nanoparticles in drug delivery: a review, Polim. Med. 48 (2018) 41–45, https://doi.org/10.17219/pim/99993.
[31] D. Morán, G. Gutiérrez, M.C. Blanco-López, A. Marefati, M. Rayner, M. Matos, Synthesis of starch nanoparticles and their applications for bioactive compound encapsulation, Appl. Sci. 11 (2021), https://doi.org/10.3390/app11104547.
[32] J. Marto, H. Ribeiro, A. Almeida, Starch-based nanocapsules as drug carriers for topical drug delivery. https://doi.org/10.1016/B978-0-12-816770-0.00017-4, 2020.
[33] N. Raghav, M.R. Sharma, J.F. Kennedy, Nanocellulose: a mini-review on types and use in drug delivery systems, Carbohydr. Polym. Technol. Appl. 2 (2021), 100031, https://doi.org/10.1016/j.carpta.2020.100031.
[34] P. Rajkumar, S. Selvaraj, S.M.O.L. Gp, Structural, optical, and magnetic studies of palladium (Pd) doped cerium oxide (CeO2) nano particles, Phys. Chem. Res. 12 (2024) 407–417.
[35] R.E. Sardjono, A.N. Fauziyah, M.D. Puspitasari, I. Musthapa, F. Khoerunnisa, G. N. Azzahra, R. Mamat, Erdiwansyah, Synthesis and antiparkinsonian activity of nanocomposite of chitosan-tripolyphosphate-Mucuna pruriens L extract (CS-TPP-MP), IOP Conf. Ser. Mater. Sci. Eng. 856 (2020) 6–12, https://doi.org/10.1088/1757-899X/856/1/012009.
[36] H.-Y. Kim, D.J. Park, J.-Y. Kim, S.-T. Lim, Preparation of crystalline starch nanoparticles using cold acid hydrolysis and ultrasonication, Carbohydr. Polym. 98 (2013) 295–301, https://doi.org/10.1016/j.carbpol.2013.05.085.
[37] E.J. Pérez-Monterroza, A.M. Chaux-Gutierrez, C.M.L. Franco, V.R. Nicoletti, Encapsulation of bixin in starch matrix using ultrasound, Ciência e Tecnol. Aliment. Pesqui. e Práticas Contemp. 1 (2021) 324–340.
[38] L. Melo-Thomas, U. Thomas, Deep brain stimulation of the inferior colliculus: a possible animal model to study paradoxical kinesia observed in some parkinsonian patients? Behav. Brain Res. 279 (2015) 1–8, https://doi.org/10.1016/j.bbr.2014.10.035.
[39] W.R. Klemm, Cholinergic-dopaminergic interactions in experimental catalepsy, Psychopharmacology (Berl) 81 (1983) 24–27, https://doi.org/10.1007/BF00439268.
[40] I. Waku, M.S. Magalhães, C.O. Alves, A.R. de Oliveira, Haloperidol-induced catalepsy as an animal model for parkinsonism: a systematic review of experimental studies, Eur. J. Neurosci. 53 (2021) 3743–3767, https://doi.org/10.1111/ejn.15222.
[41] R.E. Sardjono, F. Khoerunnisa, I. Musthopa, D. Khairunisa, P.A. Suganda, R. Rachmawati, Synthesize of zinc nanoparticles using Indonesian velvet bean (Mucuna pruriens) extract and evaluate its potency in lowering catalepsy in mice, IOP Conf. Ser. Mater. Sci. Eng. 299 (2018), https://doi.org/10.1088/1757-899X/299/1/012080.
[42] B. Divya, Study of phytochemicals in methanol extract of Mucuna pruriens, Sci. Spectra 1 (2016) 231–237.
[43] I. Ledeti, S. Bolintineanu, G. Vlase, D. Circioban, A. Ledeti, T. Vlase, L.-M. Suta, A. Caunii, M. Murariu, Compatibility study between antiparkinsonian drug Levodopa and excipients by FTIR spectroscopy, X-ray diffraction and thermal analysis, J. Therm. Anal. Calorim. 130 (2017) 433–441, https://doi.org/10.1007/s10973-017-6393-2.
[44] L. Wang, D. Su, S.N. Berry, J. Lee, Y.-T. Chang, A new approach for turn-on fluorescence sensing of l-DOPA, Chem. Commun. 53 (2017) 12465–12468, https://doi.org/10.1039/C7CC07640A.
[45] A. Subramanian, Biosynthesis and characterization of gold nanoparticle using antiparkinsonian drug Mucuna pruriens plant extract, Int. J. Res. Pharm. Sci. 1 (2010).
[46] G. Shanmugavel, G. Krishnamoorthy, Nutraceutical and Phytochemical Investigation of Mucuna Pruriens Seed, 2018, pp. 273–278.
[47] H. Sarip, M. Hossain, M. Azemi, K. Allaf, PEER-REVIEWED review article A review of the thermal pretreatment of lignocellulosic biomass towards glucose production: autohydrolysis with dic technology, Bioresources 11 (2016), https://doi.org/10.15376/biores.11.4.10625-10653.
[48] M. Ahmad, A. Gani, I. Hassan, Q. Huang, H. Shabbir, Production and characterization of starch nanoparticles by mild alkali hydrolysis and ultra-sonication process, Sci. Rep. 10 (2020) 3533, https://doi.org/10.1038/s41598-020-60380-0.
[49] N.B. Colthup, L.H. Daly, S.E. Wiberley, E.S.\& T. (Firm), Introduction to Infrared and Raman Spectroscopy, Elsevier Science, 1990.
[50] J.S. Taurozzi, V.A. Hackley, M.R. Wiesner, Ultrasonic dispersion of nanoparticles for environmental, health and safety assessment–issues and recommendations, Nanotoxicology 5 (2011) 711–729, https://doi.org/10.3109/17435390.2010.528846.
[51] R. Sardjono, N. Fauziyah, M. Puspitasari, I. Musthapa, F. Khoerunnisa, G. Azzahra, R. Mamat, E. Erdiwansyah, Synthesis and antiparkinsonian activity of nanocomposite of chitosan-tripolyphosphate- Mucuna pruriens L extract (CS-TPP-MP), IOP Conf. Ser. Mater. Sci. Eng. 856 (2020), 12009, https://doi.org/10.1088/1757-899X/856/1/012009.
[52] T.S.H. Leong, G.J.O. Martin, M. Ashokkumar, Ultrasonic encapsulation - a review, Ultrason. Sonochem. 35 (2017) 605–614, https://doi.org/10.1016/j.ultsonch.2016.03.017.
[53] S. Niranjani, C.B. Nirmala, P. Rajkumar, G. Serdaroğlu, N. Jayaprakash, K. Venkatachalam, Synthesis, characterization, biological and DFT studies of charge-transfer complexes of antihyperlipidemic drug atorvastatin calcium with Iodine, Chloranil, and DDQ, J. Mol. Liq. 346 (2022), 117862, https://doi.org/10.1016/j.molliq.2021.117862.
[54] Y.D. Yolanda, A.B.D. Nandiyanto, How to read and calculate diameter size from electron microscopy images, ASEAN J. Sci. Eng. Educ. 2 (2022) 11–36.
[55] A. Delimi, H. Ferkous, M. Alam, S. Djellali, A. Sedik, K. Abdesalem, C. Boulechfar, A. Belakhdar, K.K. Yadav, M.M.S. Cabral-Pinto, Corrosion protection performance of silicon-based coatings on carbon steel in NaCl solution: a theoretical and experimental assessment of the effect of plasma-enhanced chemical vapor deposition pretreatment, RSC Adv. 12 (2022) 15601–15612.
[56] G.H. Gaber Ahmed, A. Fernández-González, M.E. Díaz García, Nano-encapsulation of grape and apple pomace phenolic extract in chitosan and soy protein via nanoemulsification, Food Hydrocolloids 108 (2020), 105806, https://doi.org/10.1016/j.foodhyd.2020.105806.
[57] P. Rajkumar, S. Selvaraj, P. Anthoniammal, A. Ram Kumar, K. Kasthuri, S. Kumaresan, Structural (monomer and dimer), spectroscopic (FT-IR, FT-Raman, UV–Vis and NMR) and solvent effect (polar and nonpolar) studies of 2-methoxy-4-vinyl phenol, Chem. Phys. Impact. 7 (2023), 100257, https://doi.org/10.1016/j.chphi.2023.100257.
[58] S. Chen, M. Cheng, Y. Lang, C. Tian, H. Wei, C.-A. Wang, Preparation and characterization of monodispersed spherical Fe 2 O 3@ SiO 2 reddish pigments with core–shell structure, J. Adv. Ceram. 8 (2019) 39–46.
[59] L.L. Melo, P. Santos, P. Medeiros, R.O. Mello, E.A.M. Ferrari, M.L. Brandão, S. S. Maisonnette, A. Francisco, N.C. Coimbra, Glutamatergic neurotransmission mediated by NMDA receptors in the inferior colliculus can modulate haloperidol-induced catalepsy, Brain Res. 1349 (2010) 41–47, https://doi.org/10.1016/j.brainres.2010.06.020.
[60] M.L. Wadenberg, A. Soliman, S.C. VanderSpek, S. Kapur, Dopamine D(2) receptor occupancy is a common mechanism underlying animal models of antipsychotics and their clinical effects, Neuropsychopharmacol. Off. Publ. Am. Coll. Neuropsychopharmacol. 25 (2001) 633–641, https://doi.org/10.1016/S0893-133X(01)00261-5.